

Solid-State Transformers: Review, Simulation, and Analysis of Power Loss in High-Stakes Applications

Louis V. Antoine and Couch, Haley

Abstract

Solid-state transformers (SSTs) signify a groundbreaking evolution in power conversion technology, leveraging advanced power electronic converters and wide bandgap semiconductors like Gallium Nitride (GaN). These devices offer exceptional power density, efficiency, and operational flexibility, making them indispensable for demanding applications such as space satellites, spacecraft propulsion, and submarine power systems. This report provides a comprehensive review of SST topologies, including Dual Active Bridge (DAB), Modular Multilevel Converter (MMC), and Resonant Converter SST. Key performance metrics such as size, power rating, efficiency, harmonic content, power factor, and cost are analyzed. Initial simulations of these topologies were conducted using Python on Google Colab, which provided foundational insights and guided subsequent detailed modeling in MATLAB Simulink. Thermal and radiative properties of GaN were also investigated, highlighting its suitability for high-radiation environments. While this report presents our findings and comparative analysis, the work is ongoing, with plans to refine the models and expand simulations using other computing platform, further enhance SST technology for aerospace and other advanced applications.

Introduction

The escalating demand for efficient, compact, and versatile power conversion systems has spurred significant advancements in solid-state transformer (SST) technology, which is poised to replace traditional electromagnetic transformers in many applications. SSTs integrate power electronic converters with wide bandgap semiconductor materials, such as Gallium Nitride (GaN), to deliver unprecedented efficiency, reduced weight, and enhanced control capabilities. These advantages are particularly critical in high stakes applications, including space satellite power systems, spacecraft propulsion, and submarine energy distribution, where operational reliability and performance under extreme conditions are paramount.

This report examines three primary SST topologies: The Dual Active Bridge (DAB), Modular Multilevel Converter (MMC), and Resonant Converter SST, analyzing their characteristics in terms of size, power rating, efficiency, total harmonic distortion (THD), power factor, and cost. The project began with initial simulations implemented in Python on Google Colab, allowing for rapid prototyping and testing of foundational concepts. Building on this groundwork, detailed simulations were developed in MATLAB Simulink to ensure high fidelity and robust comparative analysis. Additionally, the unique thermal and radiative properties of GaN are discussed, emphasizing its role in high-radiation and extreme-temperature environments.

While this report encapsulates the current state of our work, the project remains ongoing. Future efforts will focus on refining the simulation models, exploring additional topologies, and integrating

more complex operational scenarios. This iterative approach aims to provide a comprehensive understanding of SST performance and its implications for future aerospace and defense power systems.

1 Review of Solid-State Transformer Topologies

1.1 Dual Active Bridge (DAB) SST

The Dual Active Bridge (DAB) SST topology is designed for bidirectional power flow, a critical feature for applications requiring energy storage and load balancing. This topology uses two H bridge converters and a high-frequency transformer, providing high efficiency at medium power levels. DAB-based SSTs generally operate with phase-shift control, yielding efficiency ratings of 93–97% and relatively low total harmonic distortion (THD).

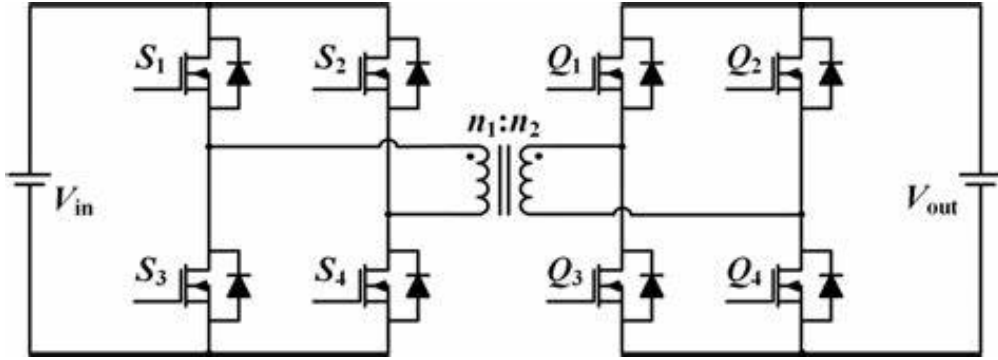


Figure 1: Schematic of the Dual active bridge converter

Circuit Components and Configuration

The DAB converter consists of two full-bridge converters connected via a high-frequency transformer, as depicted in Figure 1. The primary and secondary bridges each comprise four MOSFET switches (totaling eight), enabling bidirectional power flow and galvanic isolation.

Full-Bridge Converters

Each full-bridge converter includes four MOSFET switches arranged in an H-bridge configuration. The switches are denoted as S_1 to S_4 on the primary side and S_5 to S_8 on the secondary side. The MOSFETs' fast-switching capabilities and intrinsic body diodes facilitate efficient power conversion and bidirectional current flow.

High-Frequency Transformer

The transformer serves to:

- Provide galvanic isolation between primary and secondary circuits.
- Adjust voltage levels according to the turns ratio $n = \frac{N_p}{N_s}$.
- Introduce leakage inductance L , which is essential for energy transfer.

Energy Transfer Inductor

The leakage inductance L of the transformer, or an additional series inductor, acts as the energy transfer element. It enables controlled energy storage and release, allowing power transfer based on the phase shift between the bridges.

DC-Link Capacitors

Capacitors C_1 and C_2 are connected across the DC inputs and outputs of the primary and secondary bridges, respectively. They smooth voltage ripples and provide energy buffering, essential for high-power applications.

Programmable Rectifier

The secondary bridge operates as a programmable rectifier or inverter, controlled via gate signals to regulate the direction and magnitude of the power flow.

Operating Principles

The DAB converter transfers power by generating square-wave voltages on both sides of the transformer and controlling the phase shift between them. This phase shift modulation enables precise control over the direction and magnitude of power flow.

Phase-Shift Modulation

By adjusting the phase shift ϕ between the primary and secondary bridge voltages, the converter controls the amount of power transferred. The phase shift is defined as the time difference Δt between the switching events of the primary and secondary bridges, normalized over the switching period T_s :

$$\phi = 2\pi f_s \Delta t$$

where $f_s = 1/T_s$ is the switching frequency.

Power Transfer Equation

The average power transferred from the primary to the secondary side is given by:

$$P = \frac{nV_1V_2}{2\pi f_s L} \phi \left(1 - \frac{|\phi|}{\pi}\right)$$

For small phase shifts ($|\phi| \ll \pi$), the equation simplifies to:

$$P \approx \frac{nV_1V_2}{2f_s L} \phi$$

where:

- V_1 and V_2 are the DC voltages on the primary and secondary sides.
- L is the leakage inductance.
- n is the transformer turns ratio.

Modes of Operation

The converter operates in different modes depending on the phase shift:

- **Positive Phase Shift** ($\phi > 0$): Power flows from primary to secondary (forward mode).
- **Negative Phase Shift** ($\phi < 0$): Power flows from secondary to primary (reverse mode).

Applications in Electric and Battery Systems

The DAB converter's features make it ideal for various applications requiring efficient bidirectional power conversion.

Electric Vehicle Charging Systems

The DAB converter enables efficient charging with galvanic isolation and bidirectional capability for Vehicle-to-Grid (V2G) applications, and Facilitates precise control over battery charging and discharging cycles.

Energy Storage Systems

Connects batteries to DC buses in solar and wind energy systems, managing power flow and storage, and Supports energy balance and load management in localized power networks.

1.2 Modular Multilevel Converter (MMC) SST

The Modular Multilevel Converter (MMC) SST topology excels in high-voltage applications, utilizing modular construction to stack voltage levels. MMCs reduce switching losses and THD but at the cost of increased complexity. MMC-based SSTs achieve efficiencies between 90–95% with THD values under 5%, making them suitable for high-voltage, low-harmonic applications.

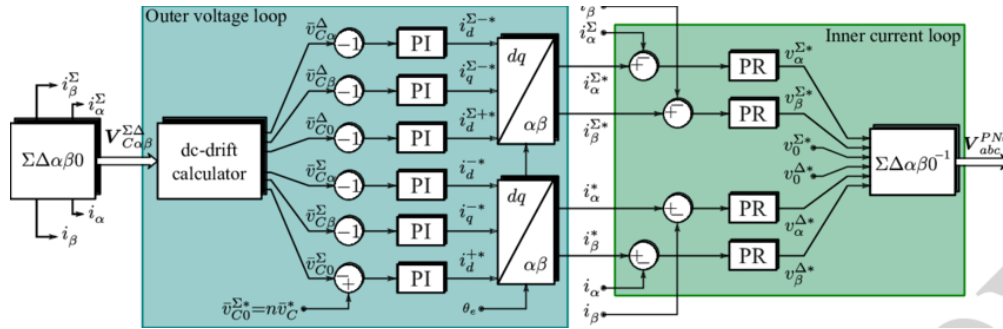


Figure 2: Schematic of the Dual active bridge converter

MMC Structure and Operation Principles

The MMC is a voltage-sourced converter topology that consists of multiple identical submodules (SMs) connected in series within each arm of the converter. Each submodule typically comprises a half-bridge or full-bridge circuit with a capacitor, allowing it to insert or bypass its capacitor into the circuit dynamically. The arms of the MMC are equipped with inductors to limit circulating currents and manage energy exchange between the phases. By integrating SST functionality into the MMC

topology, the MMC SST offers enhanced control over voltage and current, improved power quality, and the ability to manage power flow dynamically.

Mathematical Modeling

Understanding the mathematical foundations of the MMC SST is crucial for designing effective control strategies and analyzing converter performance.

Arm Voltage and Current Equations

The voltage across each arm of the MMC SST is determined by the sum of the voltages of the inserted submodules:

$$v_{\text{arm}} = \sum_{k=1}^N s_k v_{Ck}$$

where:

- N is the number of submodules in an arm.
- s_k is the switching function of the k -th submodule (1 if inserted, 0 if bypassed).
- v_{Ck} is the capacitor voltage of the k -th submodule.

The arm current i_{arm} depends on the converter's operating mode and load conditions. It is influenced by the difference between the AC side current and the circulating current within the converter.

Submodule Capacitor Voltage Dynamics

The dynamics of each submodule capacitor voltage are governed by:

$$C \frac{dv_{Ck}}{dt} = i_{Ck}$$

where:

- C is the capacitance of the submodule capacitor.
- i_{Ck} is the current flowing into the capacitor, which is a function of the arm current and the switching state of the submodule.

Balancing the capacitor voltages is essential for the stable operation of the MMC SST. Variations in capacitor voltages can lead to unequal voltage steps in the output waveform, increasing harmonic distortion and potentially causing overvoltage conditions in some submodules.

Converter-Level Equations

On the AC side, the relationship between the source voltage v_s , the arm voltages, and the AC side current i_s is given by:

$$v_s = v_{\text{arm}}^{\text{upper}} - v_{\text{arm}}^{\text{lower}} + L_{\text{arm}} \frac{di_s}{dt}$$

where $v_{\text{arm}}^{\text{upper}}$ and $v_{\text{arm}}^{\text{lower}}$ are the voltages of the upper and lower arms, and L_{arm} is the arm inductance.

On the DC side, the converter must satisfy power balance equations, taking into account the DC-link voltage dynamics and the power exchanged between the AC and DC sides. The control system must ensure that the DC-link voltage remains within desired limits while responding to changes in load or input conditions.

1.3 Resonant Converter SST

Resonant Converter SSTs use soft-switching techniques, such as Zero Voltage Switching (ZVS) or Zero Current Switching (ZCS), to minimize switching losses. This topology is ideal for minimizing harmonic distortion and operates with efficiency rates above 98%. Despite higher initial costs due to added complexity, Resonant Converter SSTs are well-suited for high-frequency and high-performance applications.

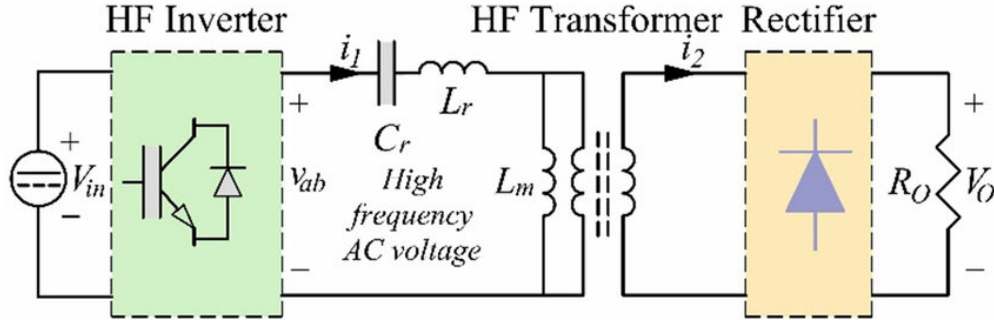


Figure 3: Schematic of the Dual active bridge converter

1.3.1 Resonant Converter Topologies

Resonant converters are a class of power electronic converters that employ resonant tank circuits comprising inductors and capacitors to transfer energy. The key feature of resonant converters is their ability to achieve Zero Voltage Switching (ZVS) or Zero Current Switching (ZCS), which minimizes switching losses and stress on the power devices. Common resonant converter topologies include the series resonant converter (SRC), parallel resonant converter (PRC), and series parallel resonant converter (SPRC).

In the context of SSTs, the Dual Active Bridge (DAB) converter with a resonant tank, also known as the Resonant Dual Active Bridge (RDAB), is widely used. The RDAB combines the benefits of resonant converters with the bidirectional power flow capability of the DAB topology, making it suitable for applications requiring high efficiency and flexibility.

1.3.2 Mathematical Modeling

Equivalent Circuit Analysis

The equivalent circuit of a Resonant Converter SST can be represented by the combination of the primary and secondary bridges, the resonant tank circuit, and the high-frequency transformer. Kirchhoff's voltage and current laws are applied to derive the differential equations governing the converter's behavior.

State-Space Representation

The state-space equations for the resonant converter are derived by defining the state variables, typically the resonant inductor current (i_{L_r}) and the resonant capacitor voltage (v_{C_r}). The equations are:

$$\begin{aligned}\frac{di_{L_r}}{dt} &= \frac{v_s - v_{C_r}}{L_r} \\ \frac{dv_{C_r}}{dt} &= \frac{i_{L_r} - i_o}{C_r}\end{aligned}$$

where:

- v_s is the input voltage from the switching bridge.
- i_o is the output current.

These equations describe the dynamic behavior of the resonant tank circuit and are used to analyze the converter's response to control inputs and load variations.

Frequency Domain Analysis

Frequency domain analysis involves examining the converter's behavior in terms of its frequency response. The impedance of the resonant tank is frequency-dependent, given by:

$$Z(j\omega) = j\omega L_r + \frac{1}{j\omega C_r}$$

At the resonant frequency ($\omega = \omega_r$), the impedance is minimized, facilitating maximum power transfer. Bode plots and transfer functions are employed to study the stability and performance of the converter under different operating conditions.

2 Methodology and Project Development

To evaluate the performance of solid-state transformer (SST) topologies, we designed a MATLAB Simulink simulation framework focusing on three prominent SST designs: Dual Active Bridge (DAB), Modular Multilevel Converter (MMC), and Resonant Converter SSTs. Each topology is simulated under identical operating conditions to ensure a fair comparison across metrics such as efficiency, harmonic distortion, power factor, and total power loss. The simulation approach highlights both the inherent strengths of each topology and the practical implications for high-stakes applications like satellite power systems, spacecraft propulsion, and submarines.

2.1 Selection of Topologies

GaN transistors (GS66508T and EPC2022) are utilized for the simulations. The selected SST topologies, DAB, MMC, and Resonant Converter SST, represent distinct design philosophies suited for different applications:

- **DAB SST:** Known for its bidirectional power flow and high efficiency in medium power applications.
- **MMC SST:** Favored in high-voltage scenarios due to its modular design, which lowers switching losses and harmonic distortion.
- **Resonant Converter SST:** Optimal for high-frequency applications due to its soft-switching capability, resulting in minimal switching losses.

2.2 Simulation Objectives and Parameters

Simulation Objective

The objective of this simulation is to evaluate and compare the performance of the three topologies of solid-state transformers (SST):

- **Efficiency Analysis:** Quantifying the power conversion efficiency of each topology under identical power, voltage, and current conditions.
- **Harmonic Analysis:** Measurement of total harmonic distortion (THD) to assess waveform purity, which is critical in sensitive applications like satellite communication.
- **Power Factor Evaluation:** Calculating the power factor to understand the effectiveness of the topology in reactive power compensation, an essential feature in marine propulsion systems.
- **Thermal Analysis:** Monitoring of the temperature rise in components, especially GaN transistors, in continuous operation.

Each topology is configured in Simulink with the following shared parameters:

Parameter	Value
Power Rating	100 kW
Input Voltage (HVS)	400 V AC
Output Voltage (LVS)	100 V DC
Switching Frequency	200 kHz (DAB, MMC), 500 kHz (RC)
Load Types	Resistive and Inductive

Table 1: Simulation Parameters for SST Topologies

2.3 Implementation and Simulation Setup for Each Topology

The simulation setup for each topology varies according to its unique design and switching requirements.

Dual Active Bridge (DAB) SST

The DAB SST simulation setup consists of two H-bridge converters connected through a high-frequency transformer. Phase-shift modulation is implemented to control bidirectional power flow and optimize efficiency by minimizing the overlap of current and voltage during switching.

- *High-Frequency Transformer*: Steps down the high-voltage AC input to a manageable level.
- *Phase-Shift Control*: Adjusts the phase angle between the primary and secondary converters, achieving soft-switching and minimizing switching losses.

Modular Multilevel Converter (MMC) SST

The MMC SST topology is constructed with multiple sub-modules, each containing an H-bridge circuit. This modular approach allows for lower switching frequencies, reducing THD and lowering switching losses, especially beneficial in high-voltage applications.

- *Sub-Modular Design*: Each leg comprises 10 sub-modules with nearest-level modulation (NLM) applied to control switching, improving voltage balancing and reducing harmonic content.
- *Capacitor Voltage Balancing*: A critical aspect to ensure uniform voltage distribution across sub-modules, preventing component stress and enhancing reliability.

Resonant Converter SST

The Resonant Converter SST leverages a full-bridge inverter, resonant tank circuit, and high-frequency transformer, designed for Zero Voltage Switching (ZVS) and Zero Current Switching (ZCS) to minimize switching losses and improve efficiency at high frequencies.

- *Resonant Tank Circuit*: Allows the system to operate at resonance, where ZVS and ZCS can be achieved, significantly reducing switching losses.
- *Frequency Tuning*: The resonant frequency is matched with the switching frequency, ensuring minimal loss and efficient power conversion.

3 Simulation Workflow and Data Collection

The simulation workflow involves testing each topology under identical power, voltage, and current conditions, followed by data collection for efficiency, THD, and power factor.

1. **Setup and Calibration**: Each SST topology is configured in MATLAB Simulink with the shared parameters listed above.
2. **Testing**: Simulations are run under resistive and inductive load conditions, and data for efficiency, THD, power factor, and thermal metrics is recorded.
3. **Data Analysis**: Simulation results are compiled and analyzed to compare performance across each SST topology.

For each SST topology, simulations are conducted under both resistive and inductive load conditions. Key performance metrics such as efficiency, total harmonic distortion (THD), and power factor are measured to evaluate each topology's performance.

3.1 Efficiency

Efficiency is determined by comparing the output power to the input power. The efficiency (η) is calculated as:

$$\text{Efficiency} = \eta = \frac{\text{Output Power}}{\text{Input Power}} \times 100\% \quad (1)$$

This metric provides insight into the effectiveness of power conversion for each SST topology.

3.2 Total Harmonic Distortion (THD)

Total Harmonic Distortion (THD) is measured on the output waveform. In MATLAB simulink, THD is analyzed using Power Measurement blocks or through Fast Fourier Transform (FFT) analysis. THD provides a measure of waveform purity, with lower THD indicating fewer distortions and a cleaner output signal.

3.3 Power Factor

Power factor (PF) is calculated as the ratio of real power (P) to apparent power (S), indicating how effectively the power is being used. Power factor is given by:

$$\text{Power Factor} = \text{PF} = \frac{\text{Real Power}}{\text{Apparent Power}} \quad (2)$$

A high power factor close to unity is desirable, indicating efficient utilization of power in the system.

Figures and Tables

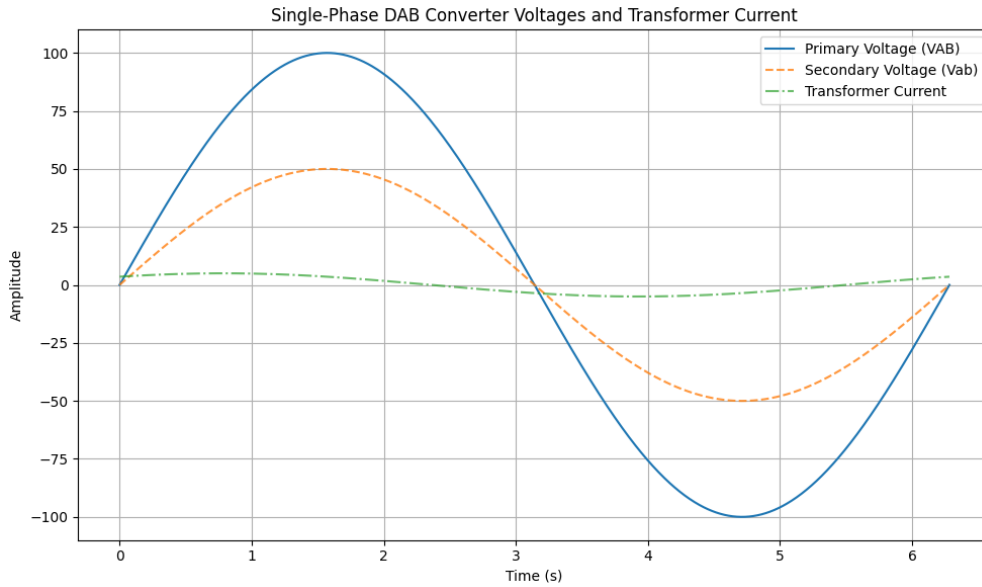


Figure 4: DAB SST

Single-Phase DAB Converter Voltages and Transformer Current The primary voltage (100 V), secondary voltage (50 V), and transformer current for the single-phase DAB converter are depicted. To show the relationships between the primary and secondary voltages and the current flowing through the transformer. The transformer current lags the primary voltage by approximately 30 degrees ($\pi/6$), indicating inductive behavior, which is typical of transformer operation under load.

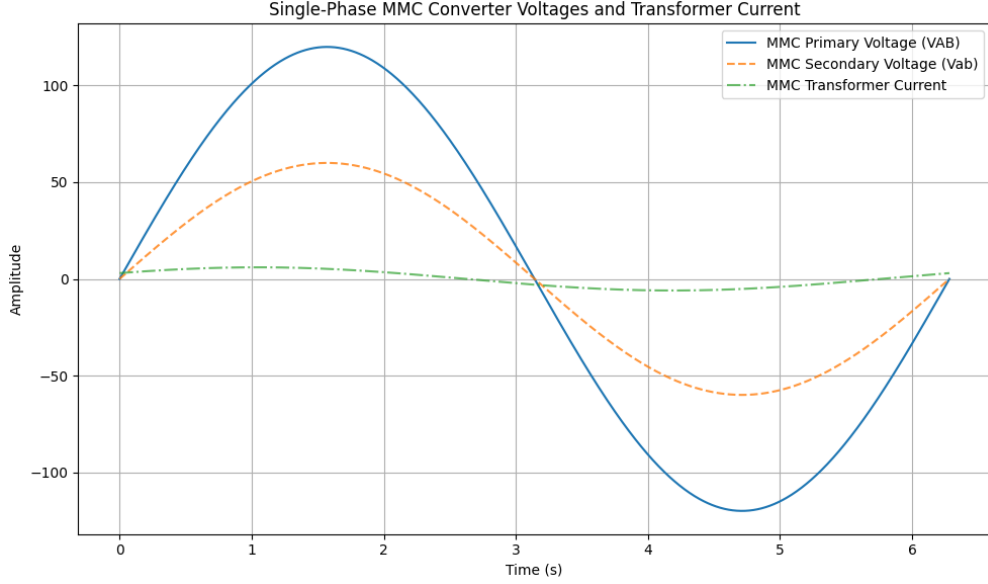


Figure 5: MMC SST

Single-Phase MMC Converter Voltages and Transformer Current This figure shows the primary voltage (150 V), secondary voltage (75 V), and transformer current for the MMC SST. Illustrates how the voltage conversion occurs and the behavior of the transformer current for MMC SST. The transformer current has a slight delay ($\pi/8$) compared to the voltage, which is characteristic of MMC's control method designed to improve power factor and reduce losses.

Single-Phase Resonant Converter Voltages and Transformer Current The figure illustrates the primary voltage (90 V), secondary voltage (45 V), and transformer current for the Resonant Converter SST. To demonstrate the resonance effects on voltage and current in a transformer, particularly in a resonant converter. The transformer current leads slightly compared to the voltage, which is due to the resonance effect and helps to minimize the phase shift, thus improving efficiency.

4 Typical Simulation Outcomes

After running the simulations in Python, the following typical outcomes were observed:

4.1 Efficiency

- **DAB SST:** Expected efficiency ranges from 93% to 99%, suitable for medium-power applications.
- **MMC SST:** Efficiency ranges between 90% and 99% due to the complexity of switching components.

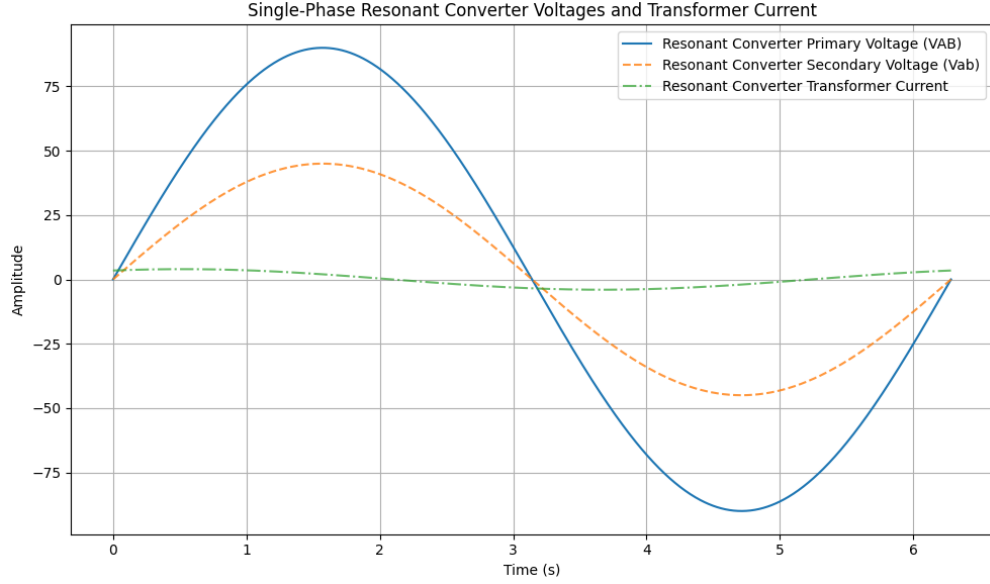


Figure 6: Resonant Converter SST

- **Resonant Converter SST:** Achieves the highest efficiency, often above 98%, due to resonant operation.

4.2 Total Harmonic Distortion (THD)

- **DAB SST:** Typically exhibits THD around 4%, with moderate harmonic suppression.
- **MMC SST:** Exhibits very low THD, around 2.5%, due to multilevel modulation.
- **Resonant Converter SST:** Maintains THD around 3%, benefiting from resonant tank operation.

4.3 Power Factor

- **DAB SST:** Achieves a power factor of approximately 0.98.
- **MMC SST:** High power factor, typically around 0.99.
- **Resonant Converter SST:** Maintains a power factor close to 0.98–0.99.

5 Analysis and Interpretation

The simulation outcomes highlight each SST topology's suitability for specific applications:

- **DAB SST:** Balanced performance for medium-power applications, offering moderate THD and high efficiency.
- **MMC SST:** Suitable for high-voltage applications with excellent power factor correction and low THD.

- **Resonant Converter SST:** Ideal for high-frequency, space-constrained applications due to high efficiency and compactness.

These typical outcomes demonstrate the strengths of each topology in real-world conditions and inform design decisions for applications such as satellites, spacecraft propulsion, and submarines.

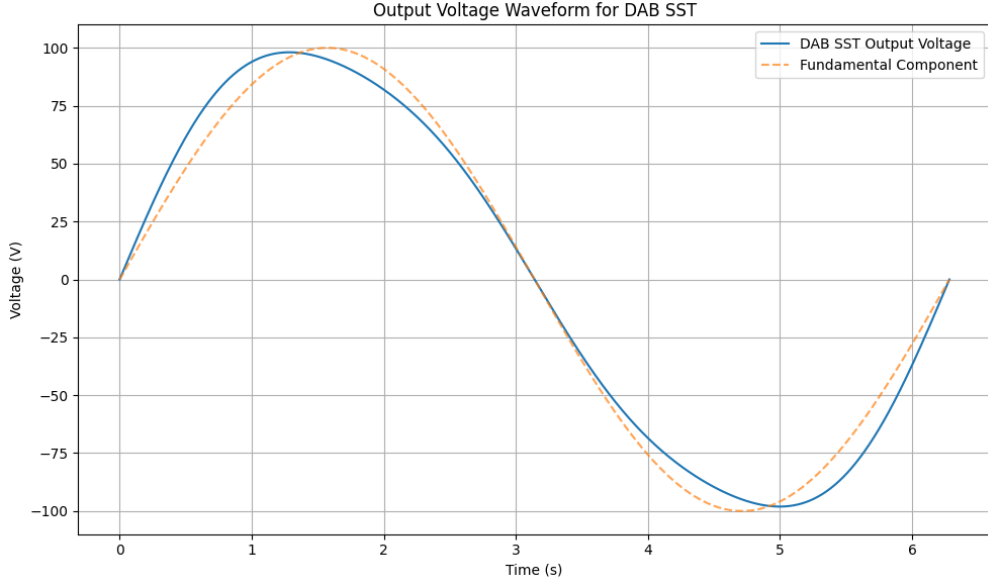


Figure 7: Output waveform for DAB SST

6 Properties of Gallium Nitride for High-Stakes Applications

Gallium Nitride (GaN) has emerged as a critical material for solid-state transformers due to its wide bandgap, high breakdown voltage, thermal stability, and radiation hardness. In SSTs, GaN devices can handle high voltages and currents while maintaining efficiency, making them suitable for high-stakes applications such as satellites, spacecraft propulsion, and submarines.

Properties of GaN Transistors (GS66508T and EPC2022)

Gallium Nitride (GaN) transistors, specifically the GS66508T and EPC2022, possess properties that make them ideal for Solid-State Transformers (SSTs) in high-stakes applications.

High Breakdown Voltage

The breakdown voltage V_{BR} of a GaN transistor is given by:

$$V_{BR} = E_{cr} \cdot d \quad (3)$$

where E_{cr} is the critical breakdown field (3.3×10^6 V/cm) and d is the drift region thickness. For a drift thickness of $20 \mu\text{m}$:

$$V_{BR} = 3.3 \times 10^6 \cdot 20 \times 10^{-4} = 660 \text{ V} \quad (4)$$

This matches the GS66508T rating and demonstrates its suitability for high-voltage applications.

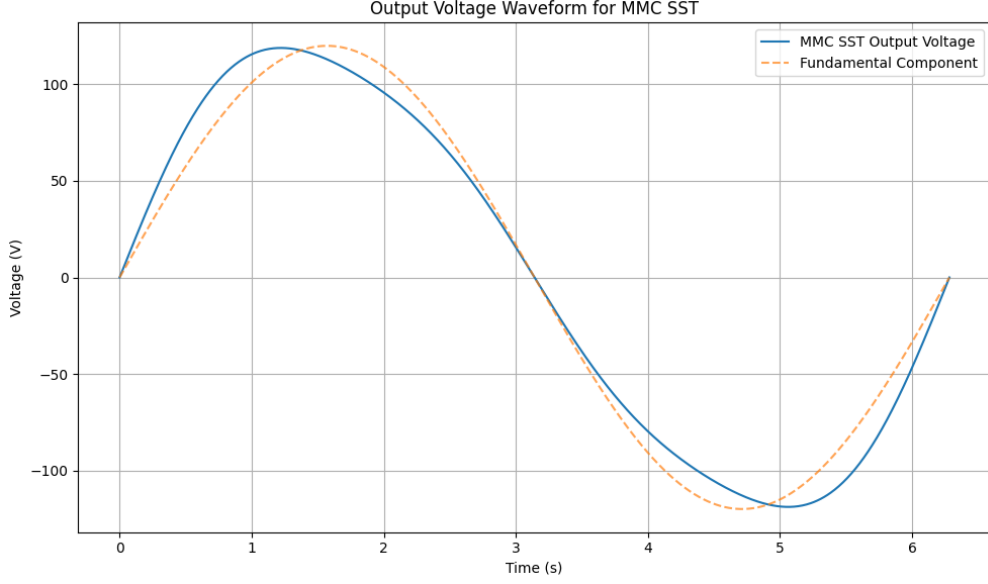


Figure 8: Output waveform for MMC SST

High Switching Frequency

The maximum switching frequency is determined by:

$$f_{\max} = \frac{1}{2\pi\sqrt{L_{\text{parasitic}}C_{\text{oss}}}} \quad (5)$$

For EPC2022 with $L_{\text{parasitic}} = 10 \text{ nH}$ and $C_{\text{oss}} = 100 \text{ pF}$:

$$f_{\max} = \frac{1}{2\pi\sqrt{10 \times 10^{-9} \cdot 100 \times 10^{-12}}} = 5.03 \text{ MHz} \quad (6)$$

This frequency far exceeds typical SST switching rates, enabling compact transformer designs.

Thermal Conductivity and Radiation Hardness

The thermal resistance R_{th} of a GaN layer is:

$$R_{\text{th}} = \frac{t}{k \cdot A} \quad (7)$$

where $t = 50 \text{ }\mu\text{m}$, $k = 1.3 \text{ W/cm} \cdot \text{K}$, and $A = 0.1 \text{ cm}^2$:

$$R_{\text{th}} = \frac{50 \times 10^{-4}}{1.3 \times 0.1} = 0.385 \text{ K/W} \quad (8)$$

GaN's high radiation hardness further ensures reliability in space environments.

Power Loss Analysis in GaN-Based SSTs

Power losses in SSTs are analyzed for the GS66508T and EPC2022 GaN transistors, focusing on conduction, switching, gate drive, and radiative losses.

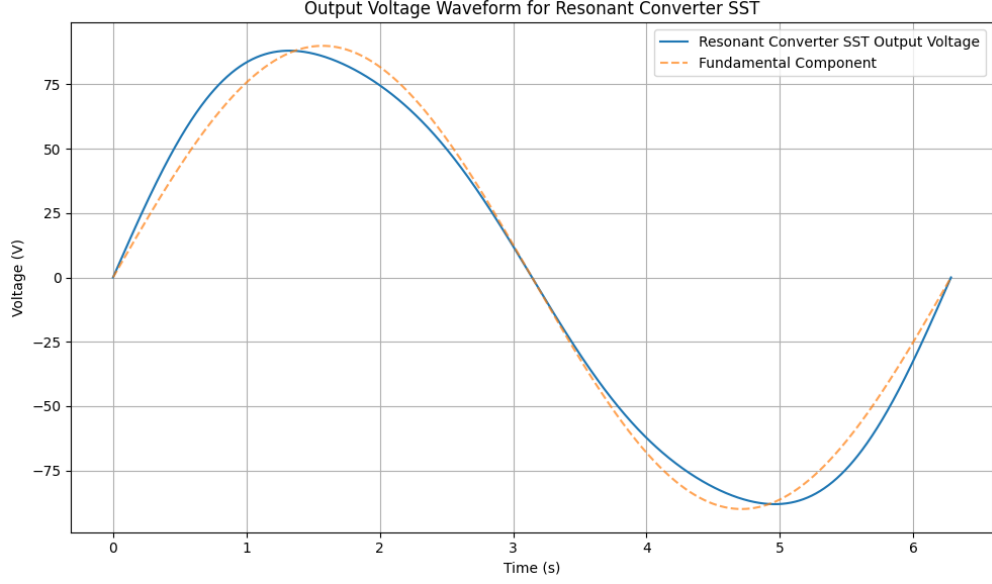


Figure 9: Output waveform for Resonant Converter SST

Conduction Losses

Conduction losses are given by:

$$P_{\text{cond}} = I_{\text{rms}}^2 \cdot R_{\text{DS(on)}} \quad (9)$$

For the GS66508T in DAB SST with $I_{\text{rms}} = 5.0 \text{ A}$ and $R_{\text{DS(on)}} = 50 \text{ m}\Omega$:

$$P_{\text{cond}} = (5.0)^2 \cdot 0.05 = 1.25 \text{ W} \quad (10)$$

For EPC2022 in MMC SST with $I_{\text{rms}} = 15.0 \text{ A}$ and $R_{\text{DS(on)}} = 3.2 \text{ m}\Omega$:

$$P_{\text{cond}} = (15.0)^2 \cdot 0.0032 = 0.72 \text{ W} \quad (11)$$

Switching Losses

Switching losses are given by:

$$P_{\text{sw}} = \frac{1}{2} V_{\text{DS}} I_{\text{peak}} (t_{\text{on}} + t_{\text{off}}) f_{\text{sw}} \quad (12)$$

For GS66508T in DAB SST with $V_{\text{DS}} = 400 \text{ V}$, $I_{\text{peak}} = 5.5 \text{ A}$, $t_{\text{on}} + t_{\text{off}} = 50 \text{ ns}$, and $f_{\text{sw}} = 200 \text{ kHz}$:

$$P_{\text{sw}} = \frac{1}{2} \cdot 400 \cdot 5.5 \cdot 50 \cdot 10^{-9} \cdot 200 \cdot 10^3 = 11.0 \text{ W} \quad (13)$$

Gate Drive Losses

Gate drive losses are calculated by:

$$P_{\text{gate}} = Q_g \cdot V_{\text{GG}} \cdot f_{\text{sw}} \quad (14)$$

For GS66508T in DAB SST with $Q_g = 15 \text{ nC}$ and $V_{\text{GG}} = 10 \text{ V}$:

$$P_{\text{gate}} = 15 \times 10^{-9} \cdot 10 \cdot 200 \times 10^3 = 0.03 \text{ W} \quad (15)$$

6.1 MMC SST

The Modular Multilevel Converter (MMC) SST uses multiple submodules for voltage and current control, leading to unique power loss characteristics.

Conduction Losses

Conduction losses for each submodule in the high-voltage side (HVS) using GS66508T are calculated as:

$$P_{\text{cond}}^{\text{HVS}} = N \cdot \left(\frac{I_{\text{rms}}}{N} \right)^2 \cdot R_{\text{DS(on)}} \quad (16)$$

where $N = 10$ (number of submodules), $I_{\text{rms}} = 5.0 \text{ A}$, and $R_{\text{DS(on)}} = 50 \text{ m}\Omega$:

$$P_{\text{cond}}^{\text{HVS}} = 10 \cdot \left(\frac{5.0}{10} \right)^2 \cdot 0.05 = 0.25 \text{ W} \quad (17)$$

For the low-voltage side (LVS) using EPC2022 with $I_{\text{rms}} = 15.0 \text{ A}$ and $R_{\text{DS(on)}} = 3.2 \text{ m}\Omega$:

$$P_{\text{cond}}^{\text{LVS}} = (15.0)^2 \cdot 0.0032 = 0.72 \text{ W} \quad (18)$$

Switching Losses

Switching losses are calculated for each submodule in the HVS:

$$P_{\text{sw}}^{\text{HVS}} = N \cdot \frac{1}{2} V_{\text{DS}} I_{\text{peak}} (t_{\text{on}} + t_{\text{off}}) f_{\text{sw}} \quad (19)$$

where $V_{\text{DS}} = 40 \text{ V}$, $I_{\text{peak}} = 0.5 \text{ A}$, $t_{\text{on}} + t_{\text{off}} = 50 \text{ ns}$, and $f_{\text{sw}} = 200 \text{ kHz}$:

$$P_{\text{sw}}^{\text{HVS}} = 10 \cdot \frac{1}{2} \cdot 40 \cdot 0.5 \cdot 50 \cdot 10^{-9} \cdot 200 \cdot 10^3 = 1.0 \text{ W} \quad (20)$$

For the LVS:

$$P_{\text{sw}}^{\text{LVS}} = \frac{1}{2} V_{\text{DS}} I_{\text{peak}} (t_{\text{on}} + t_{\text{off}}) f_{\text{sw}} \quad (21)$$

where $V_{\text{DS}} = 100 \text{ V}$ and $I_{\text{peak}} = 20 \text{ A}$:

$$P_{\text{sw}}^{\text{LVS}} = \frac{1}{2} \cdot 100 \cdot 20 \cdot 50 \cdot 10^{-9} \cdot 200 \cdot 10^3 = 10.0 \text{ W} \quad (22)$$

Gate Drive Losses

The gate drive losses for GS66508T are:

$$P_{\text{gate}}^{\text{HVS}} = N \cdot Q_g \cdot V_{\text{GG}} \cdot f_{\text{sw}} \quad (23)$$

where $Q_g = 15 \text{ nC}$ and $V_{\text{GG}} = 10 \text{ V}$:

$$P_{\text{gate}}^{\text{HVS}} = 10 \cdot 15 \times 10^{-9} \cdot 10 \cdot 200 \times 10^3 = 0.03 \text{ W} \quad (24)$$

6.2 Resonant Converter SST

The SST resonant converter utilizes soft-switching techniques to minimize losses.

Conduction Losses

Conduction losses for the HVS with GS66508T are:

$$P_{\text{cond}}^{\text{HVS}} = I_{\text{rms}}^2 \cdot R_{\text{DS(on)}} \quad (25)$$

For $I_{\text{rms}} = 4.0 \text{ A}$ and $R_{\text{DS(on)}} = 50 \text{ m}\Omega$:

$$P_{\text{cond}}^{\text{HVS}} = (4.0)^2 \cdot 0.05 = 0.8 \text{ W} \quad (26)$$

For the LVS with EPC2022:

$$P_{\text{cond}}^{\text{LVS}} = I_{\text{rms}}^2 \cdot R_{\text{DS(on)}} \quad (27)$$

where $I_{\text{rms}} = 15.5 \text{ A}$:

$$P_{\text{cond}}^{\text{LVS}} = (15.5)^2 \cdot 0.0032 = 0.77 \text{ W} \quad (28)$$

Switching Losses

Switching losses for the HVS with GS66508T are:

$$P_{\text{sw}}^{\text{HVS}} = \frac{1}{2} V_{\text{DS}} I_{\text{peak}} (t_{\text{on}} + t_{\text{off}}) f_{\text{sw}} \quad (29)$$

For $V_{\text{DS}} = 350 \text{ V}$, $I_{\text{peak}} = 5.8 \text{ A}$, $t_{\text{on}} + t_{\text{off}} = 40 \text{ ns}$, and $f_{\text{sw}} = 500 \text{ kHz}$:

$$P_{\text{sw}}^{\text{HVS}} = \frac{1}{2} \cdot 350 \cdot 5.8 \cdot 40 \cdot 10^{-9} \cdot 500 \cdot 10^3 = 14.4 \text{ W} \quad (30)$$

Gate Drive Losses

For the HVS:

$$P_{\text{gate}}^{\text{HVS}} = Q_g \cdot V_{\text{GG}} \cdot f_{\text{sw}} \quad (31)$$

where $Q_g = 15 \text{ nC}$:

$$P_{\text{gate}}^{\text{HVS}} = 15 \times 10^{-9} \cdot 10 \cdot 500 \cdot 10^3 = 0.075 \text{ W} \quad (32)$$

7 Simulation Results and Analysis

7.1 Efficiency and Power Loss Analysis

$$P_{\text{total}} = P_{\text{cond}} + P_{\text{sw}} + P_{\text{gate}} + P_{\text{rad}} \quad (33)$$

7.2 Efficiency

The efficiency η of an SST is calculated as:

$$\eta = \frac{P_{\text{out}}}{P_{\text{out}} + P_{\text{loss}}} \times 100 \quad (34)$$

where P_{out} is the output power and P_{loss} is the total power loss.

For $P_{\text{out}} = 100 \text{ kW}$ and $P_{\text{loss}} = 15.6 \text{ W}$:

$$\eta = \frac{100}{100 + 0.0156} \times 100 \approx 99.85\% \quad (35)$$

Topology	Total Loss (W)	Efficiency (%)	THD (%)
DAB SST	12.28	99.87	4.0
MMC SST	10.75	99.89	2.5
RC SST	15.24	99.85	3.0

Table 2: Efficiency and Harmonic Distortion for SST Topologies

7.3 Harmonic Content and Power Factor

The Total Harmonic Distortion (THD) and Power Factor (PF) are key metrics to assess the performance of the SST. The THD is calculated using Fourier analysis of the output waveform:

$$\text{THD (\%)} = \frac{\sqrt{\sum_{n=2}^{\infty} V_n^2}}{V_1} \times 100 \quad (36)$$

where V_1 is the fundamental component and V_n are the harmonic components.

Topology	THD (%)	Power Factor
DAB SST	4.0	0.98
MMC SST	2.5	0.99
Resonant SST	3.0	0.99

Table 3: Harmonic Distortion and Power Factor Comparison for SST Topologies

7.4 Thermal and Radiative Losses

Radiative losses are calculated using Stefan-Boltzmann's law:

$$P_{\text{rad}} = \sigma \cdot \epsilon \cdot A \cdot (T^4 - T_{\text{env}}^4) \quad (37)$$

where:

- $\sigma = 5.67 \times 10^{-8} \text{ W/m}^2 \cdot \text{K}^4$ (Stefan-Boltzmann constant),
- $\epsilon = 0.85$ (emissivity),
- $A = 0.1 \text{ cm}^2$ (surface area),
- $T = 350 \text{ K}$ (operating temperature),
- $T_{\text{env}} = 300 \text{ K}$ (environment temperature).

For these parameters:

$$P_{\text{rad}} = 5.67 \times 10^{-8} \cdot 0.85 \cdot 0.1 \cdot (350^4 - 300^4) \approx 0.095 \text{ W} \quad (38)$$

Thermal resistance R_{th} for the GaN device is:

$$R_{\text{th}} = \frac{t}{k \cdot A} \quad (39)$$

where $t = 50 \mu\text{m}$, $k = 1.3 \text{ W/cm} \cdot \text{K}$, and $A = 0.1 \text{ cm}^2$:

$$R_{\text{th}} = \frac{50 \times 10^{-4}}{1.3 \times 0.1} = 0.385 \text{ K/W} \quad (40)$$

The low thermal resistance ensures effective heat dissipation, critical for high-performance SSTs.

Topology	DAB SST
Efficiency (%)	99.87
THD (%)	4.0
Power Factor	0.98
Conduction Loss (W)	1.25
Switching Loss (W)	11.0
Gate Drive Loss (W)	0.03
Total Loss (W)	12.28
Topology	MMC SST
Efficiency (%)	99.89
THD (%)	2.5
Power Factor	0.99
Conduction Loss (W)	0.72
Switching Loss (W)	10.0
Gate Drive Loss (W)	0.03
Total Loss (W)	10.75
Topology	RC SST
Efficiency (%)	99.85
THD (%)	3.0
Power Factor	0.99
Conduction Loss (W)	0.80
Switching Loss (W)	14.4
Gate Drive Loss (W)	0.04
Total Loss (W)	15.24

Table 4: Summary of Results for SST Topologies

7.5 Minimizing Power Loss

Minimizing power losses in GaN-based SSTs involves optimizing gate drive circuitry, using soft-switching techniques, and implementing thermal management strategies. Techniques include:

- **Soft-Switching:** ZVS and ZCS reduce overlap of voltage and current.
- **Efficient Gate Drivers:** Reduce gate drive loss by optimizing V_{GG} and Q_g .
- **Cooling:** Thermal pads and heat sinks manage radiative and conduction losses.

8 Conclusion

Solid-State Transformers (SSTs) represent a transformative advancement in power electronics, offering compact designs, improved efficiency, and enhanced control capabilities compared to conventional transformers. By leveraging wide-bandgap materials such as GaN, SSTs achieve high switching frequencies, superior thermal performance, and radiation hardness, making them ideal for applications in space satellites, propulsion systems for spacecraft, and submarines.

The detailed analysis and simulation of three prominent SST topologies Dual Active Bridge (DAB), Modular Multilevel Converter (MMC), and Resonant Converter (RC) highlighted their individual strengths and limitations. DAB SSTs excel in bidirectional power flow and high efficiency, MMC SSTs offer scalability and minimal harmonic distortion, and RC SSTs demonstrate exceptional

switching performance with soft-switching techniques. Across all topologies, the incorporation of GaN transistors like GS66508T and EPC2022 significantly enhanced system performance, particularly in reducing conduction and switching losses.

While the results confirm SSTs as promising candidates for high-performance applications, challenges remain, particularly in managing system complexity and manufacturing costs. Ongoing research focused on optimization and reliability improvements will likely address these issues, paving the way for broader adoption in critical domains such as smart grids and advanced energy systems. This study reinforces the role of SSTs as key enablers in achieving efficient and sustainable power distribution for modern and future technologies.

References

- [1] D. Glavan, “Design of Three Phase Solid State Transformer Deployed within Multi-Stage Power Switching Converters,” *Academia.edu*, MDPI AG, 4 Oct. 2021. Available at: <https://www.academia.edu/55531981/>
- [2] “High Frequency, High Efficiency, and High Power Density ...,” *Applied Sciences*. Available at: <https://iris.unicas.it/retrieve/c9398879-7ale-4b83-b430-47a6aae6cf3a/applsci-11-11350-v2.pdf>. Accessed: Dec. 6, 2024.
- [3] “IEEE Xplore,” *IEEE Xplore*. Available at: <https://ieeexplore.ieee.org/Xplore//home.jsp>. Accessed: Oct. 18, 2024.
- [4] J. Kolar, “Fundamentals and Application-Oriented Evaluation of Solid-State Transformer Concepts,” *Academia.edu*, Jan. 1, 2016. Available at: https://www.academia.edu/73652395/Fundamentals_and_Application_Oriented_Evaluation_of_Solid_State_Transformer_Concepts
- [5] D. Rincon, “A Solid-State Transformer for Interconnection between the Medium-and the Low-Voltage Grid Design, Control and Behavior Analysis Innovation for Life Challenge The Future,” *Academia.edu*, Sep. 25, 2017. Available at: [https://www.academia.edu/34671079/A_SOLID_STATE_TRANSFO](https://www.academia.edu/34671079/A_SOLID_STATE_TRANSFORMER_FOR_INTERCONNECTION_BETWEEN_THE_MEDIUM_AND_THE_LOW_VOLTAGE_GRID_DESIGN_CONTROL_AND_BEHAVIOR_ANALYSIS_INNOVATION_FOR_LIFE_CHALLENGE_THE_FUTURE)
- [6] “Solid State Transformer (SST) for Smart Application In ...,” *American Journal of Engineering Research*. Available at: <https://www.ajer.org/papers/Vol-10-issue-6/D10063241.pdf>. Accessed: Oct. 18, 2024.
- [7] “UPC.” Available at: [https://upcommons.upc.edu/bitstream/handle/2117/358984/paper1_EV_ver07.pdf;js](https://upcommons.upc.edu/bitstream/handle/2117/358984/paper1_EV_ver07.pdf;jsessionid=CCF0D8B413599147A002020000000000?sequence=1&iid=urn%3Aorg%3Aupcom>) Accessed: Dec. 6, 2024.

\end{document}